Ionic Motion and Phase Transition in Potassium Hydrogendifluoride KHF_2 Studied by Pulsed NMR

Yoshihiro FURUKAWA* and Hideko KIRIYAMA
The Institute of Scientific and Industrial Research, Osaka University, Yamadakami, Suita 565

(Received May 8, 1978)

Nuclear spin-lattice relaxation times, T_1 and $T_{1\rho}$, have been measured above room temperature for ^1H and ^{19}F nuclei in powdered KHF_2 and its deuterated analogue. Below 400 K and in the high-temperature β-phase (T_t=469.8 K), the magnetization recovery for both nuclei in KHF_2 is strongly non-exponential owing to the heteronuclear H–F interaction. In the low-temperature α-phase the T_1 *vs.* $1/T$ curves show broad minima ascribable to the 180°-flip motion of linear $[FHF]^-$ anions. The activation energy E_a of this motion was determined to be 50.5±2 kJ/mol. The phase transition, which is defined by discontinuous changes in both T_1 and $T_{1\rho}$, is associated with diffusional disorder superimposed on rapid isotropic reorientation of the HF_2^- ion. The relaxational process in the β-phase is governed by self-diffusion of the anions with an E_a of 80±6 kJ/mol deduced from the $T_{1\rho}$ data. In contrast to the earlier suggestion from electrical measurements, the NMR results indicate that the dominantly mobile species in the conducting high-temperature β-phase are not single F^- ions but complex $[FHF]^-$ anions.

Potassium hydrogendifluoride KHF_2 has been studied extensively by diffraction, spectroscopic and other physical methods, on account of its hydrogen bond forming unique difluoride ion $[F\cdots H\cdots F]^-$. In all cases, except for early infrared studies, the HF_2^- ion was found to be linear and centro-symmetric with an unusually short F–F distance of 2.29 Å.[1-6]

The compound KHF_2 is tetragonal with cell constants a=5.672, c=6.801 Å and Z=4 in the room-temperature α-phase.[3] The linear HF_2^- ions are arranged in planes (001). In these planes the $[FHF]^-$ ionic axes are directed alternately parallel to either [110] or $[\bar{1}10]$. At the transition temperature T_t (196.7 °C), the crystal transforms to the cubic β-phase. This is accompanied by large changes in volume and entropy, the cell constants being a=6.36 Å and Z=4.[1,7,8] In the high-temperature phase the F–F axis may orient parallel to any of the four body-diagonals [111] of the cubic cell with equal probability to attain higher symmetry. It seemed worthwhile to clarify whether such a disordered structure is dynamic or static by means of nuclear magnetic resonance (NMR) techniques.

Also of interest is the fact that the ionic conductivity of the compound increases sharply at T_t by about two orders of magnitude, when T_t is approached from a low temperature.[9,10] This strongly suggests that dynamical disorder or migration of ions takes place in the β-phase. Furthermore, electromotive force and electrolysis experiments show that the F^- ions contribute dominantly to the ionic conduction in the high-temperature phase.[11]

The purpose of this study is to determine the type of molecular motion associated with phase transition and ionic conduction by measuring proton and fluorine NMR relaxation times. Kriger *et al.* have reported the spin-lattice relaxation times, T_1, of KHF_2[12] and $CsHF_2$.[13] Our independent experiments, however, include a more detailed study of the temperature dependence of T_1 and the rotating-frame relaxation time, $T_{1\rho}$, in KHF_2 and its deuterated analogue. The results and discussion presented here disagree to some extent with those of Kriger *et al.*

Experimental

Commercial potassium hydrogendifluoride was twice recrystallized from water and dried over P_2O_5. Deuterated KDF_2 was prepared by repeated crystallization from saturated heavy-water solutions of the salt in a closed bottle. Polyethylene wares were used in order to avoid the reaction of HF acid with silicate glass. For the NMR measurement on the α-phase the powdered KHF_2 was placed in an 8 mm diam. glass tube, which was evacuated and then sealed. When the sample was kept below T_t for several days, the wall of the tube was hardly corroded at all by gaseous HF, but when the sample was transformed to the waxy β-phase, it became corroded at the contact surface. For the relaxation measurements on the β-phase, several pieces of single crystals with dimensions of about 4×4×1 mm^3 were wrapped in Teflon tape and then sealed in a glass tube. It was thought that the use of Teflon would not interfere with the measurements since the ^{19}F FID (free induction decay) signal in the β-phase is long as compared with that in Teflon. Actually, the Teflon coated sample gave almost the same relaxation data as those of the sample coated with vacuum-pump-oil. The samples used were identified from the X-ray powder patterns at room temperature before and after NMR measurements. No extra diffraction peaks, especially those assignable to crystalline KF, were recognized after the sample had been heated at about 500 K for ten hours.

T_1 and $T_{1\rho}$ were measured with a Bruker pulsed NMR spectrometer B-KR 322s by the conventional methods. The Larmor frequencies were 20 and 18.814 MHz for ^1H and ^{19}F, respectively. Since the FID signal in the α-phase was very short, its height was obtained from the solid echo[14] and was averaged on a NIC 1074 signal averager. The sample temperature controlled within ±1 K was measured with a copper-constantan thermocouple.

Results and Discussion

The proton and fluorine relaxation times of KHF_2 are summarized in Fig. 1 as a semilogarithmic plot *versus* inverse temperature. Below 400 K the T_1 behavior for both nuclei was somewhat complicated by the presence of heteronuclear H–F interactions. In the region below the temperatures of the T_1 minima, the relaxations of ^1H and ^{19}F became markedly non-

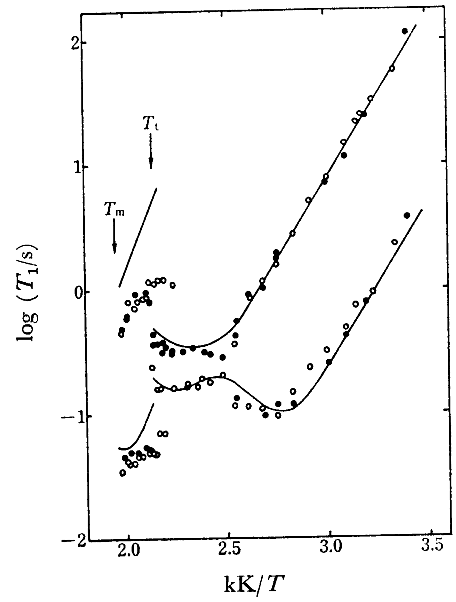

Fig. 1. Temperature dependences of the spin-lattice relaxation times, T_1, in KHF_2. ●: ^1H, ○: ^{19}F. Below 400 K and in the β-phase two components of T_1 are shown because of the non-exponential magnetization recovery. The solid lines in the α-phase are calculated on the basis of a model of 180°-flipping HF_2^- ions.

exponential. Each recovery curve of magnetization was manually resolved into two components, one of which (the short component) was characterized by a short relaxation time T_1', and the other by a long relaxation time T_1''.[15] As shown in Fig. 1, the relaxations for ^1H and ^{19}F have the same pair of T_1' and T_1'' below 400 K. On the other hand, at temperatures between 400 K and T_t (469.8 K), both relaxations are nearly exponential, the minimum value of T_1(H) being about twice as long as that of T_1(F). The results differ from those of Kriger *et al.*[12] as regards (1) the non-exponential behavior, (2) the absence of a temperature region in which $T_1(H)<T_1(F)$, and (3) the slope of log T_1 *vs.* $1/T$ curve in the high-temperature β-phase.

T_1 in the α-Phase of KHF_2. In this system, since the heteronuclear dipole interaction between ^1H and ^{19}F cannot be neglected, the observed relaxation rates of both nuclei are the eigenvalues of the following relaxation matrix:[15,16]

$$\begin{pmatrix} R_{HH}+R_{HF} & R_{HF}' \\ R_{FH}' & R_{FF}+R_{FH} \end{pmatrix} \tag{1}$$

The element R_{HF} represents the proton relaxation rate *via* the dipolar interaction between ^1H and ^{19}F spins. The relative magnitudes of these matrix elements are expected to govern the non-exponential behavior and the depths of the T_1 minima for ^1H and ^{19}F.[15]

$T_{1\,\mathrm{min}}(F)<T_{1\,\mathrm{min}}(H)$ indicates that $(R_{FF}+R_{FH})>(R_{HH}+R_{HF})$, suggesting that the two-fold reorientation or 180° flip of HF_2^- ions takes place rapidly in the α-phase. Look and Lowe derived a formula for the relaxation rate of flipping water molecules in a hydrated single crystal.[17] It is also applicable to R_{FF} in the case of 180°-flipping HF_2^- ions. Thus, we obtain

$$R_{FF}=\frac{3\gamma_F{}^4\hbar^2I_F(I_F+1)}{16N}\sum_{i\neq j}\Bigg[\eta^1_{ij}\frac{\tau_f}{1+0.25\omega_{0F}{}^2\tau_f{}^2}$$
$$+(2\xi^1_{ij}+\eta^2_{ij})\frac{\tau_f}{1+\omega_{0F}{}^2\tau_f{}^2}+2\xi^2_{ij}\frac{\tau_f}{1+4\omega_{0F}{}^2\tau_f{}^2}\Bigg], \tag{2a}$$

$$\eta^q_{ij}=\frac{1}{2}|\chi^q_{ij}(\beta\beta)+\chi^q_{ij}(\delta\delta)-\chi^q_{ij}(\beta\delta)-\chi^q_{ij}(\delta\beta)|^2, \tag{2b}$$

$$\xi^q_{ij}=|\chi^q_{ij}(\beta\beta)-\chi^q_{ij}(\delta\delta)|^2+|\chi^q_{ij}(\beta\delta)-\chi^q_{ij}(\delta\beta)|^2, \tag{2c}$$

where the symbols are those of Look and Lowe.[17] Since our sample was powdered, Eq. 2 was used after spatial averaging.[18]

On the other hand, the relaxation rate due to the heteronuclear H–F interactions was derived for a flipping model, in which the central H atom is fixed and each terminal F atom jumps between two equilibrium lattice sites. Only its spatially averaged form is presented here:

$$R_{HF}=\gamma_H{}^2\gamma_F{}^2\hbar^2/40\sum_F[r_{HF}(\beta)^{-6}+r_{HF}(\delta)^{-6}-r_{HF}(\beta)^{-3}r_{HF}(\delta)^{-3}$$
$$\times(3\cos^2\Delta_{\beta\delta}-1)]g(\omega_{0H},\omega_{0F},\tau_f), \tag{3a}$$

$$R_{HF}'=\gamma_H{}^2\gamma_F{}^2\hbar^2/40\sum_F[r_{HF}(\beta)^{-6}+r_{HF}(\delta)^{-6}-r_{HF}(\beta)^{-3}r_{HF}(\delta)^{-3}$$
$$\times(3\cos^2\Delta_{\beta\delta}-1)]g'(\omega_{0H},\omega_{0F},\tau_f), \tag{3b}$$

$$g(\omega_{0H},\omega_{0F},\tau_f)=\frac{\tau_f}{1+(\omega_{0H}-\omega_{0F})^2\tau_f{}^2}+\frac{3\tau_f}{1+\omega_{0H}{}^2\tau_f{}^2}$$
$$+\frac{6\tau_f}{1+(\omega_{0H}+\omega_{0F})^2\tau_f{}^2}, \tag{3c}$$

$$g'(\omega_{0H},\omega_{0F},\tau_f)=-\frac{\tau_f}{1+(\omega_{0H}-\omega_{0F})^2\tau_f{}^2}$$
$$+\frac{6\tau_f}{1+(\omega_{0H}+\omega_{0F})^2\tau_f{}^2}. \tag{3d}$$

Symbols β and δ denote the two possible sites for a given F atom and $\Delta_{\beta\delta}$ the angle between two H–F vectors of $r_{HF}(\beta)$ and $r_{HF}(\delta)$. It can readily be shown from the atomic arrangements that $R_{HH}=0$, whereas the other components are $R_{FH}=(1/2)R_{HF}$ and $R_{FH}'=(1/2)R_{HF}'$.[16]

The summation was taken over 14 neighboring HF_2^- ions about a central HF_2^- ion in Eq. 2, and over 6 neighbors in Eq. 3, within the tetragonal structure. Diagonalizing Eqs. 1—3 and using the Arrhenius relation, we can calculate the temperature dependences of T_1(H) and T_1(F). Simulated T_1 curves are represented by the solid lines in Fig. 1, with an activation energy E_a of 50.5 kJ/mol deduced from the linear region on the low-temperature side of the $T_{1\,\mathrm{min}}$. Agreement between the observed and calculated $T_{1\,\mathrm{min}}$ values indicates that the 180°-flip motion of the $[FHF]^-$ ion is responsible for the T_1 process in the α-phase. On the low-temperature side of $T_{1\,\mathrm{min}}$, the off-diagonal elements in the relaxation matrix become comparable in magnitude with the diagonal elements, as anticipated from the non-exponential behavior. On the other hand, above and near the temperature of $T_{1\,\mathrm{min}}$ both relaxations for ^1H and ^{19}F are exponential, since the off-diagonal elements can be neglected in comparison with the diagonal elements. The 180°-flip motion of linear $[FHF]^-$ ions was also found in $CsHF_2$.[13] The activation energy E_a of 50.5 kJ/mol for KHF_2 is much larger than that of 14.9 kJ/mol for $CsHF_2$. The room-temperature phase of $CsHF_2$ (T_t=61 °C) is isomorphous with the α-phase of KHF_2, but the cell dimensions of the former are appreciably larger than those of the latter. Thus, the difference in E_a is attributable primarily to the cation-size effect.

T_1 and $T_{1\rho}$ in the β-Phase of KHF_2. At the phase transition both T_1 and $T_{1\rho}$ change abruptly, the FID signals of ^1H and ^{19}F becoming very long as in a liquid above T_t. The T_2 value defined as the time necessary for the FID to fall to 1/e of its initial value is of the order of a millisecond, demonstrating that the HF_2^- ions are very mobile. Thus, the static disordered model is excluded in view of motional narrowing. The T_1 and $T_{1\rho}$ data for the β-phase are given in Fig. 2 against an expanded scale of inverse temperature. The magnetization recovery for the T_1 process again becomes nonexponential, but not that for the $T_{1\rho}$ process. This is in line with the positive and negative slopes of the T_1 and $T_{1\rho}$ *vs.* $1/T$ curves, respectively. As shown in Fig. 2, the β-phase was often supercooled down to 445 K, some indication on the $T_{1\rho}$ minimum being recognized in the supercooled region.

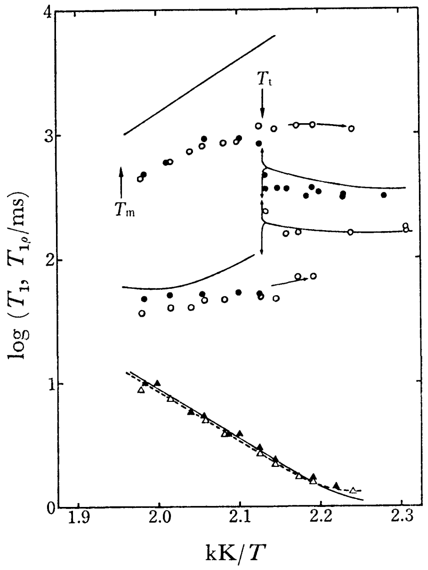

Fig. 2. The T_1 and $T_{1\rho}$ in the β-phase of KHF_2, plotted against an expanded scale of inverse temperature. ●: ^1H T_1, ○: ^{19}F T_1, ▲: ^1H $T_{1\rho}$ (H_1=10 G), △: ^{19}F $T_{1\rho}$ (H_1=10.6 G). The solid and broken lines represent the calculated ^1H and ^{19}F $T_{1\rho}$ curves, respectively. The self-diffusion of the HF_2^- ions is assumed. The phase transition and thermal hysteresis are indicated by arrows.

The dominant relaxation mechanism in the high-temperature phase cannot be assigned to isotropic reorientation of HF_2^- ions, since the experimental second moments estimated from the FID shapes are much smaller than the calculated ones for this model. The primary process is ascribable to the self-diffusion of HF_2^- ions. The rate of process is usually calculated by means of correlation functions derived and tabulated by Torrey[19] and Sholl.[20] Their derivations involve only the homonuclear dipole interactions for a random walk model, where jumping motion occurs between the nearest-neighbor sites. In the case of KHF_2, however, the interactions are complicated since they include the heteronuclear H–F as well as the H–H and F–F interactions, the magnitudes of which are comparable.

For the sake of simplicity, we start from an approximate expression to analyze the relaxation and correlation times for the diffusion process. In the temperature region where $T_1 > T_{1\rho}$, the $T_{1\rho}$ can be approximated by the following equation:[15]

$$T_{1\rho}(\mathrm{I})^{-1} = \frac{2}{3}\gamma_{\mathrm{I}}^2 M_{\mathrm{II}}\left(\frac{3}{2}\,\frac{\tau_{\mathrm{d}}}{1+4\omega_{1\mathrm{I}}^2\tau_{\mathrm{d}}^2}\right) + \frac{1}{2}\gamma_{\mathrm{I}}^2 M_{\mathrm{IS}}\left\{\frac{2\tau_{\mathrm{d}}}{1+\omega_{1\mathrm{I}}^2\tau_{\mathrm{d}}^2}+\frac{1}{2}\,\frac{\tau_{\mathrm{d}}}{1+(\omega_{0\mathrm{I}}-\omega_{0\mathrm{S}})^2\tau_{\mathrm{d}}^2}\right\}, \tag{4}$$

where subscripts I and S stand for H and F or *vice versa*, and M_{IS} is the second moment of the I-spin absorption spectrum due to I–S dipolar interaction prior to diffusional narrowing.

The motion of a linear $[FHF]^-$ ion would be expected to be thermally activated in the sequence of the 180° flip, the isotropic reorientation, and the diffusion with an increase in temperature. In the present case, however, the reorientational motion could not be separated from the other motions; it was probably prevented by the occurrence of the phase transition. On this supposition the values of the second moments in Eq. 4 were taken as those calculated for the rapid isotropic reorientation of the HF_2^- ions. The second moments were estimated on the basis of the NaCl-type structure of the β-phase and using the approximation that the two fluorine atoms of each HF_2^- ion are effectively located at the center of the ion; they are $M_{HH}=0.626$, $M_{HF}=0.491$, $M_{FF}=1.105$, and $M_{FH}=0.278\ G^2$.

By substituting these values into Eq. 4 and by taking an activation energy of 80 kJ/mol from the experimental $T_{1\rho}$ *vs.* $1/T$ curve, the temperature dependence of the ^1H and ^{19}F $T_{1\rho}$'s was simulated. The results together with the corresponding T_1' and T_1'' are shown in Fig. 2. The agreement between the calculated and experimental curves for both $T_{1\rho}$'s supports the relaxation model used in the present analysis. On the other hand, the experimental curves for T_1' and T_1'' are significantly depressed from the calculated ones; the departure increases with decreasing temperature in the β-phase. This indicates that the rapid reorientation and the slow diffusional motion are superposed in this region. The correlation time for the reorientation is roughly estimated to be 10^{-12} s at the transition point. The motional parameters are summarized in Table 1.

TABLE 1. SUMMARY OF RELAXATIONAL PARAMETERS

Phase	E_a/(kJ mol^{-1})	τ_0/s	Motion
α-Phase	50.5±2	6.4×10^{-15}	180° flip
β-Phase	80 ±6	5×10^{-16}	diffusion

T_1 and $T_{1\rho}$ in KDF_2. In order to confirm the relaxation mechanism, the T_1 and $T_{1\rho}$ of ^{19}F were measured on deuterated KDF_2 (Fig. 3). Since the isotope exchange of ^1H with ^2H nuclei almost extinguishes the heteronuclear dipole interaction, the relaxa-

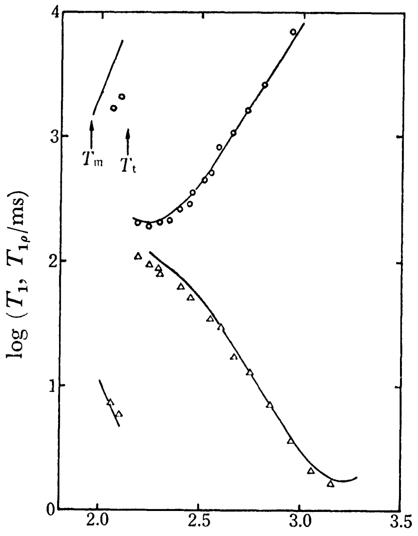

Fig. 3. Temperature dependences of T_1 and $T_{1\rho}$ for ^{19}F in KDF_2 ($H_1 = 10.6$ G). The solid lines represent the expected dependences based on relaxation processes similar to those in KHF_2 (see text).

tion becomes exponential for all temperatures studied. The T_1 value in the α-phase of KDF_2 is nearly equal to the long component T_1'' (Fig. 1). The $T_{1\,\mathrm{min}}$ value is only 1.2 times that for ^{19}F in KHF_2. This shows that the T_1'' in KHF_2 is mainly due to the F–F dipolar interaction; of course both are modulated by 180°-flipping of the HF_2^- ion. Therefore, the T_1 and $T_{1\rho}$ values were calculated from Eq. 2 and the corresponding formulae derived by Look and Lowe,[17] respectively, using the same values as those found in KHF_2, except $\tau_0 = 7 \times 10^{-15}$ s. The results are shown by solid lines in Fig. 3. Agreement between the calculated and experimental T_1 and $T_{1\rho}$ curves furnishes additional evidence for the relaxation due to the flipping of the HF_2^- ion.

On the other hand, the ^{19}F relaxation times in the β-phase of KDF_2 were markedly affected by the isotope exchange, *viz.*, $T_1(KDF_2) \approx 2 \times T_1''(KHF_2)$ and $T_{1\rho}(KDF_2) \approx 2 \times T_{1\rho}(KHF_2)$. The calculation based on Eq. 4, taking $M_{FH} = 0$, supports the results. However, the absolute value of the ^{19}F T_1 in the β-phase is in poor agreement with the experimental one, possibly for the same reason as that for KHF_2.

Phase Transition. At the phase transition the relaxation times change discontinuously with accompanying thermal hysteresis. This suggests a first-order phase transition. The compounds containing linear XY_2^- ions are often transformed into cubic phases at high temperatures. The azides of rubidium and caesium have the same structure as that of KHF_2 at room temperature, *viz.*, a tetragonally distorted CsCl-type structure with space group I4/mcm. On heating, the azides undergo phase transitions to cubic Pm3m phases.[21] Such I4/mcm-Pm3m transition involves a small displacement of the anion. The transition entropies of 7.9 for Rb- and 7.5 J/(K mol) for Cs-azides were interpreted in terms of random orienting N_3^- ions parallel to three cube-edges. Caesium hydrogendifluoride also shows an I4/mcm-Pm3m transition having a transition entropy of 8.4 J/(K mol), which is nearly equal to the expected $R\ln 3$.[22]

On the other hand, the phase transition of KHF_2 is somewhat different from those described above. The high-temperature β-phase has an NaCl-type structure with space group Fm3m, and the HF_2^- ions are directed at random along four body-diagonals. The I4/mcm-Fm3m transition is associated with a large ionic displacement as well as disordering of the HF_2^- ions, as evidenced from the large increase in volume at the transition point.[8] The present NMR study on KHF_2 and KDF_2 suggests that the rapid flip motion triggers the phase transition and the spherical reorientation of the linear HF_2^- ion causes the symmetry of the anion to be effectively cubic in the β-phase. However, the diffusive motion of the HF_2^- ion can also be correlated with the I4/mcm-Fm3m transition, since the transition entropy of 23.8 J/(K mol),[7] is much larger than $R\ln 4$ expected for pure orientational disorder in the β-phase.

Mobile Ions in the β-Phase. A number of hydrogen-bonded crystals have been studied as proton conductors with special interest centering on the identity of charge carriers and the mechanism of ionic migration.[23] The ionic conduction in KHF_2, where the hydrogen atom is located inside an isolated anion, becomes substantial only in the high-temperature β-phase. Bruinink and Kosmeijer determined the ionic transport numbers from changes in chemical composition on electrolysis as follows: $t_F \approx 0.75$, $t_K \approx 0.25$, and $t_H \approx 0$ in the β-phase, while $t_H \approx 1$ in the α-phase.[11] They explained the relatively high conductivity in the β-phase in terms of the migration of F^- (and to a smaller extent K^+) ions but not of H^+ ions.

The results of ^1H and ^{19}F T_1 are evidence for self-diffusion of the ions in the conducting β-phase, affording valuable information on the mobile ion-species. If the hydrogen ions are essentially immobile in this phase, as suggested from the electrolysis experiments, then the calculated $T_{1\rho}$ for ^1H should be about two times that for ^{19}F except near the $T_{1\rho}(H)$ minimum. The estimation is not compatible with the observation that $T_{1\rho}(H) \approx T_{1\rho}(F)$. Thus, the HF_2^- ion diffuses as a whole; at least H^+ and F^- ions move with almost equal correlation times, which is not in agreement with the results of electrolysis. On the other hand, the activation energy (80 kJ/mol) for the self-diffusion found from the NMR study is in fairly good agreement with the value of 86 kJ/mol deduced from the electric conductivity measurements.[10] Both values are much smaller than the hydrogen-bond energy, 240 kJ/mol, estimated for $[F\cdots H\cdots F]^-$ ions.[24] It can be concluded that the most mobile charge carriers in the conducting high-temperature β-phase are not single F^- ions but complex $[FHF]^-$ anions.

The authors are grateful to Professor Emeritus Ryôiti Kiriyama for his continued interest and stimulating discussions. This work was partly supported by a Grant-in-Aid for Scientific Research from the Ministry of Education (No. 047076).

References

1) R. Kruh, K. Fuwa, and T. E. McEver, *J. Am. Chem. Soc.*, **78**, 4256 (1956).

2) J. A. Ibers, *J. Chem. Phys.*, **40**, 402 (1964).

3) H. L. Carrell and J. Donohue, *Israel J. Chem.*, **10**, 195 (1972).

4) J. S. Waugh, F. B. Humphrey, and D. M. Yost, *J. Phys. Chem.*, **57**, 486 (1953).

5) J. C. Pratt and J. A. S. Smith, *J. Chem. Soc., Faraday Trans. 2*, **71**, 596 (1975).

6) P. Van Hecke, H. W. Spiess, and V. Haeberlen, *J. Magn. Reson.*, **22**, 93 (1976).

7) M. L. Davis and E. F. Westrum, Jr., *J. Am. Chem. Soc.*, **65**, 338 (1961).

8) R. W. Fink and E. F. Westrum, Jr., *J. Phys. Chem.*, **60**, 800 (1956).

9) J. M. Pollock and M. Sharan, *J. Chem. Phys.*, **47**, 4064 (1967).

10) J. Bruinink and G. H. J. Broers, *J. Phys. Chem. Solids*, **33**, 1713 (1972).

11) J. Bruinink and B. Kosmeijer, *J. Phys. Chem. Solids*, **34**, 897 (1973).

12) Yu. G. Kriger, N. K. Moroz, and S. P. Gabuda, *Fiz. Tverd. Tela*, **18**, 891 (1976) [*Sov. Phys. Solid State*, **18**, 514 (1976)].

13) Yu. G. Kriger, S. P. Gabuda, and N. K. Moroz, *Fiz, Tverd. Tela*, **17**, 3420 (1975) [*Sov. Phys. Solid State*, **17**, 2239 (1976)].

14) J. G. Powles and J. H. Strange, *Proc. Phys. Soc.*, **82**, 6 (1963).

15) D. E. O'Reilly, E. M. Peterson, and T. Tsang, *Phys. Rev.*, **160**, 333 (1967).

16) A. Abragam, "The Principles of Nuclear Magnetism," Oxford Univ. Press, (1961), Chap. 8.

17) D. C. Look and I. J. Lowe, *J. Chem. Phys.*, **44**, 2995 (1966).

18) K. Sagisawa, H. Kiriyama, and R. Kiriyama, *Bull. Chem. Soc. Jpn.*, **51**, 1942 (1978).

19) H. C. Torrey, *Phys. Rev.*, **92**, 962 (1953); **96**, 690 (1954).

20) C. A. Sholl, *J. Phys. C*, **7**, 3378 (1974); **8**, 1737 (1975); W. A. Barton and C. A. Sholl, *ibid.*, **9**, 4315 (1976).

21) H. J. Mueller and J. A. Joebstl, *Z. Kristallogr., Kristallgeom., Kristallphys., Kristallchem.*, **121**, S385 (1965).

22) A. J. C. White and C. W. F. T. Pistorius, *J. Chem. Phys.*, **56**, 4318 (1972).

23) L. Glasser, *Chem. Rev.*, **75**, 21 (1975).

24) T. C. Waddington, *Trans. Faraday Soc.*, **54**, 25 (1958); W. Van Gool, J. Bruinink, and P. H. Bottelberghs, *J. Inorg. Nucl. Chem.*, **34**, 3631 (1972).